Down regulation of QKI triggers ferroptosis by interfering cytoskeletal stability and lipid membrane integrity in double negative prostate cancer

Cheol Keun Park

Department of Medicine

The Graduate School, Yonsei University

Down regulation of QKI triggers ferroptosis by interfering cytoskeletal stability and lipid membrane integrity in double negative prostate cancer

Cheol Keun Park

Department of Medicine

The Graduate School, Yonsei University

Down regulation of QKI triggers ferroptosis by interfering cytoskeletal stability and lipid membrane integrity in double negative prostate cancer

Directed by Professor Nam Hoon Cho

The Doctoral Dissertation
submitted to the Department of Medicine
the Graduate School of Yonsei University
in partial fulfillment of the requirements
for the degree of Doctor of Philosophy

Cheol Keun Park

December 2021

This certifies that the Doctoral Dissertation of Cheol Keun Park is approved.

Thesis Supervisor: Nam Hoon Cho

Thesis Committee Member#1: Young-Deuk Choi

Thesis Committee Member#2: Ho Kyung Seo

Thesis Committee Member#3: Hyunho Han

Thesis Committee Member#4: Yong Mee Cho

The Graduate School
Yonsei University

December 2021

ACKNOWLEDGEMENTS

First of all, I would like show my gratitude to my supervisor, Professor Nam Hoon Cho, for giving me inspiring advice and support for preparing this thesis and setting a role model for me by his passionate devotion for pathology.

Also, I would like to express my gratefulness to professor Young-Deuk Choi, Ho Kyung Seo, Hyunho Han and Yong Mee Cho for invaluable advice, instruction and careful concern for completing this article.

Lastly, I deeply thank my dearest family and my colleagues for their consistent support and care.

<TABLE OF CONTENTS>

LIST OF FIGURES

LIST OF TABLES

ABSTRACT

Down regulation of QKI triggers ferroptosis by interfering cytoskeletal stability and lipid membrane integrity in double negative prostate cancer

Cheol Keun Park

Department of Medicine
The Graduate School, Yonsei University

(Directed by Professor Nam Hoon Cho)

The widespread application of androgen deprivation therapy for the recurrent or metastatic prostate cancer triggers the emergence of double negative prostate cancer (DNPC). Despite aggressive behavior of DNPC, few targeted therapy has been established compared to androgen receptor positive prostate cancer (ARPC). This study revealed that the application of statin can trigger ferroptosis in DNPC represented by overexpression of RNA-binding protein quaking (QKI). PC3 and DU145 cells were selected as DNPC model and showed overexpression of QKI. MicroRNA-200 family, especially miR-200b, repressed QKI expression in PC3 cells. After overexpressing QKI in ARPC cell lines, the enhancement of stemness was observed. High expression of rho GDP-dissociation inhibitor, myosin phosphatase rho interacting protein and integrin beta 4 was associated with high QKI expression on immunohistochemistry of prostate cancer specimens. As a therapeutic target of QKI, fluvastatin was selected and treated to QKI-overexpressing (QKI-OE) cells. The treated QKI-OE cells showed diminished proliferation and increased intracellular reactive oxygen species, suggesting the occurrence of ferroptosis. In Kaplan-Meier analysis, shorter progression free survival was identified in DNPC and cases with high QKI expression ($P < 0.001$ for all). When

combining DNPC and QKI expression, DNPC with high QKI expression showed worst prognosis ($P < 0.001$). In conclusion, QKI was overexpressed in DNPC and associated with inferior prognosis. QKI-OE tumor cells were selectively sensitive to fluvastatin, which triggers ferroptosis. Application of statin that targets QKI can be the therapeutic option for the DNPC patients.

Key words: double negative prostate cancer, quaking, ferroptosis, statin, miR-200b

Down regulation of QKI triggers ferroptosis by interfering cytoskeletal stability and lipid membrane integrity in double negative prostate cancer

Cheol Keun Park

Department of Medicine
The Graduate School, Yonsei University

(Directed by Professor Nam Hoon Cho)

I. INTRODUCTION

Androgen deprivation therapy (ADT) is the first-line treatment for the recurrent or metastatic prostate cancer, where androgen receptor (AR) is a tumorigenic driver.[1] After the application of ADT, the resistant phenotype of prostate cancer, which is called castration-resistant prostate cancer (CRPC) has emerged. Among CRPC, double negative prostate cancer (DNPC) shows distinct characteristics, which lacks of AR and neuroendocrine (NE) marker expression.[2,3] In addition, DNPC cell line showed increased expression of integrin beta 4 (ITGB4),[3] which is associated with stemness feature in breast cancer.[4] Despite aggressive behavior of DNPC, few targeted therapy has been established compared to AR positive prostate cancer (ARPC).

Recent study reported ferroptosis inducers, erstin and RSL3, as a novel therapeutic strategy in advanced prostate cancer.[5] Ferroptosis is a form of regulated cell death, which is triggered by iron-dependent accumulation of lipid hydroperoxides.[6] Glutathione peroxidase 4 (GPX4) eliminates lipid hydroperoxides and acts as a regulator of ferroptosis. Several pathways and molecules, such as amino acid, iron, lipid metabolism, glutathione synthesis and coenzyme Q10, are related to the execution of

ferroptosis.[6,7] Statin, one of the several inducers related to the pathways of ferroptosis, depletes coenzyme Q10 and inhibits biosynthesis of GPX4 via prohibiting downstream tRNA isopentenylation.[8,9] In addition, recent study reported that several microRNAs including miR-638 suppresses FTH1 and triggers intracytoplasmic iron accumulation.[10]

Lipid metabolism regulates ferroptosis via several pathways. Several enzymes such as acyl-CoA synthetase long-chain family member 4 (ACSL4), lysophosphatidylcholine acyltransferase 3 and 15-lipoxygenase catalyzes the peroxidation of polyunsaturated fatty acids (PUFAs) and triggers ferroptosis.[11] On the contrary, activated exogenous monounsaturated fatty acids (MUFAs) by ACSL3 displaces PUFAs from plasma membrane and reduces the sensitivity of cell to ferroptosis.[12] A recent study reported the impaired synthesis of MUFAs in quaking (QKI) knockout mice, suggesting the regulatory role QKI in lipid synthesis.[13]

Besides the regulatory role of lipid synthesis, QKI regulates the metabolism of adipose tissue itself. In adipose tissue, the knockdown of QKI promotes brown fat energy dissipation and transformation of white fat to brown fat, causing thermogenesis. On the contrary, the induction of QKI mediated by cAMP-cAMP response element binding protein axis restricts the energy consumption by interfering mRNA stabilization and translation of *UCP1* and *PGC1α*, the key thermogenic genes in adipose tissue.[14]

QKI also regulates several processes of RNA metabolism such as mRNA splicing, circular RNA formation and miRNA stabilization.[15-17] Via alterative splicing, QKI plays an important role in cardiac sarcomerogenesis and contractile function.[18] In cancers, QKI promotes epithelial-to-mesenchymal transition (EMT) through increasing circular RNA.[15] Several actin cytoskeleton-associated genes, including *MPRIP* and *MYOF* are directly targeted by both QKI and miR-200c, revealing coordinated control of alternative splicing and mRNA abundance during EMT in breast cancer.[19] However, a recent study has reported QKI also represses EMT in head and neck cancer via negative feedback loop to maintain homeostasis of EMT-inducing signals.[20] On the contrary, QKI functions as tumor suppressor in several types of cancers such as colon, stomach, and lung cancer.[21-23] Especially, via epistatic interaction with *TP53*, QKI

suppresses the tumorigenesis by stabilizing miR-20a in glioblastoma.[24]

Despite several studies about DNPC, QKI and ferroptosis, the role of QKI and correlation with ferroptosis in DNPC has not been fully elucidated. Thus, this study tried to investigate the role of QKI and ferroptosis in the progression and treatment of DNPC.

II. MATERIALS AND METHODS

1. Cell culture

LNCaP, MDA-PCa-2B, PC3, DU145 and RWPE-1 cell lines were purchased from American Type Culture Collection. LNCaP, PC3 and DU145 cells were maintained in RPMI-1640 (Gibco, Grand Island, NY, USA) supplemented with 10% fetal bovine serum (FBS) at 37°C in 5% CO_2. MDA-PCa-2B cell was maintained in BRFF-HPC1 (Athena Environmental Sciences, Baltimore, MD, USA) supplemented with 10% FBS at 37°C in 5% CO_2. RWPE-1 was maintained in Keratinocyte serum-free medium (Gibco) supplemented with human recombinant epidermal growth factor (Gibco) and bovine pituitary extract (Gibco) under recommended conditions. Cells were fed twice weekly and split weekly with trypsinization.

2. RNA isolation and microRNA microarray

Total RNA was isolated using TRIzol reagent (Invitrogen, Carlsbad, CA, USA) according to the manufacturer’s protocol. The quality of RNA was confirmed using an Agilent 2100 Bioanalyzer (Agilent Technologies, Santa Clara, CA, USA). MicroRNA microarrays were performed using the Agilent Human miRNA v14 (Agilent Technologies) according to the manufacturer's instructions. The target prediction of miRNAs was surveyed using TargetScan database (https://www.targetscan.org).

3. RNA-sequencing data analysis

Cancer cell line RNA-sequencing dataset was acquired from Cancer Cell Line

Encyclopedia (CCLE). Weil-Cornell Medicine[25] and Stand Up to Cancer/Prostate Cancer Foundation (SU2C-PCF)[26] dataset for castration-resistant neuroendocrine carcinoma/adenocarcinoma were downloaded from cBioPortal for Cancer Genomics (https://www.cbioportal.org). AR activity score and NE signature score were calculated as previously described.[2] Expression values of mRNAs and microRNAs in each dataset was transformed to Z-score ((sample value – population mean)/sample standard deviation), used to generate gene set score. The cut-off for negative correlations between miRNA and gene pairs was defined as Pearson's correlation coefficient < -0.25.

4. Western blot

After cell lysis with a PRO-PREP kit (iNtRON Biotechnology, Seongnam, Republic of Korea), protein extracts were centrifuged at 15,000 × g for 15 min. Twenty micrograms protein was electrophoresed on 10% polyacrylamide gels and transferred onto a nitrocellulose membrane (Bio-Rad, Hercules, CA, USA). After blocking with 5% skim milk for 1 h at room temperature, probing was performed with primary antibody against QKI (dilution 1:5000, polyclonal, Bethyl Laboratories, Montgomery, TX, USA). Glyceraldehyde 3 phosphate dehydrogenase (dilution 1:500, clone 0411, Santa Cruz Biotechnology, Santa Cruz, CA, USA) was used as an internal control. After blocking the blotted membrane with 0.5% bovine serum albumin for 1 hour at room temperature, incubation with secondary antibody against mouse (SA001) and rabbit (SA002, GenDEPOT, Barker, TX, USA) was performed. Visualization was performed by enhanced chemiluminescence detection kit (GenDEPOT).

5. microRNA and siRNA transfection

Silencer negative control siRNA and QKI siRNA were transfected using Lipofectamine 2000 (Invitrogen). Appropriate MISSION miRNA mimics (nontargeting miRNA, miR-141, miR-200a, miR-200b, miR-200c, and miR-494; Sigma Aldrich, St. Louis, MO, USA) were transfected using X-tremeGENE 360 Transfection Reagent (Sigma

Aldrich).

6. Production of QKI overexpressing cell lines

QKI-overexpressing (QKI-OE) prostate cancer cell lines were generated by infecting QKI-lentiviral activation particles (Santa Cruz Biotechnology), using a synergistic activation mediator transcription activation system designed to specifically and efficiently upregulate gene expression via lentiviral transduction of cells.[27] Briefly, cells were incubated with the target virus particle or control activation particle for 24 hours with Polybrene (Sigma Aldrich). Infected cells were selected by puromycin for 96 hours. Overexpression of QKI was confirmed western blot.

7. Sphere formation assay

To create tumor sphere, METHOCEL (Sigma Aldrich) and Matrigel (BD Biosciences, Franklin Lakes, NJ, USA) were used as previously described.[20] Then, the mixture of tumor sphere was implanted in the center of each well of a 12-well plate. After polymerization of gels, each well was filled with culture media.

8. Aldehyde dehydrogenase (ALDH) detection assay

ALDH activity was measured by using the ALDEFLUOR ALDH assay kit (STEMCELL Technologies, Cambridge, MA, USA) according to the manufacturer's protocol as previously described.[28] In brief, cells were resuspended in ALDEFLUOR buffer and incubated with the ALDH substrate. As a negative control, cells was also incubated with diethylaminobenzaldehyde, an ALDH inhibitor. After 35 to 40 minutes of incubation at 37°C, cells were analyzed with FACSCalibur flow cytometer (BD Biosciences). Results were presented as percentages of ALDH active (ALDHbr) cells.

9. *In silico* drug screening

DepMap data of multiple cancer cell lines CRISPR screen (https://depmap.org) and Cancer Therapeutic Response Portal (CTRP) database[29] was used for *in silico* drug

screening to identify the sensitive drug for QKI. In DepMap database, CERES score of each gene according to each cell line was obtained. In CTRP database, the area under curve (AUC) of each drug based on each cell line was obtained. The lower AUC indicated the more sensitive the cell is to the drug of interest. These two datasets were merged by using cell line names as identifier. Then a similarity matrix using Pearson correlation metric were generated. This new drug sensitivity–gene dependency score matrix contained all matched correlation coefficients for corresponding drug and gene (481 drugs, 17634 genes).

10. Intracellular reactive oxygen species (ROS) measurement

Intracellular ROS was evaluated by using 2,7′-dichlorodihydrofluorescein diacetate (H_2DCFDA; Invitrogen). Cells were treated with the H_2DCFDA for 10 min, and then washed twice with phosphate buffered saline (PBS). Fluorescence of cells in PBS was measured using the FACSCalibur flow cytometer (BD Biosciences).

11. Patient selection

The consecutive 72 prostate cancer patients which showed disease progression after the application of ADT were selected as CRPC group. After matching International Society of Urological Pathology (ISUP) grade group and pathological tumor staging based on the 8th American Joint Committee on Cancer (AJCC) criteria to CRPC patients, 83 ADT-naïve consecutive radical prostatectomy (RP) specimen between 2006 and 2011 were selected as ADT-naive prostate cancer (ADT-naïve PC). All clinicopathologic parameters, including age at the diagnosis, serum cholesterol level, body mass index (BMI), histologic subtype, Gleason score, ISUP grade group, tumor volume, presence of extraprostatic extension (EPE), seminal vesicle involvement (SVI), lymphovascular invasion (LVI) and resection margin (RM) involvement and pathological tumor, node and metastasis (TNM) staging based on the 8th AJCC criteria were obtained from medical record review.

All cases were periodically followed and checked for loco-regional recurrence

or metastasis by imaging and prostate specific antigen (PSA) evaluation. The first postoperative PSA was obtained 6–8 weeks after the operation. Biochemical recurrence (BCR) was defined as a postoperative PSA equal to or more than 0.2 ng/mL. Cases with BCR or the evidence of locoregional recurrence or distant metastasis by image study or pathologic confirmation were defined as those with disease progression. Progression free survival (PFS) was defined as the time from the date of the first curative operation to the date of the first disease progression or to the date of death without disease progression.

12. Immunohistochemistry (IHC) and interpretation

Four-µm tissue sections from formalin fixed paraffin embedded blocks were used for immunohistochemistry. IHC was performed using the Ventana Benchmark XT automated staining system (Ventana Medical Systems, Tucson, AZ, USA), according to the manufacturer's protocol. Cell Conditioning 1 buffer (EDTA, pH 8.0, Ventana Medical Systems) was used for antigen retrieval. The sections were incubated with primary antibody for AR (prediluted, clone SP107, Cell Marque, Rocklin, CA, USA), CD56 (dilution 1:100, clone CD564, Novocastra, Newcastle upon Tyne, UK), synaptophysin (dilution 1:450, clone DAK-SYNAP, DAKO, Glostrup, Denmark), chromogranin A (dilution 1:500, clone DAK-A3, DAKO), p53 (dilution 1:300, clone DO-7, Novocastra), PTEN (dilution 1:200, clone D4.3, Cell Signaling Technology, Danvers, MA, USA), QKI (dilution 1:500), integrin beta 4 (dilution 1:200, polyclonal, Atlas Antibodies, Bromma, Sweden), myosin phosphatase rho interacting protein (MPRIP; dilution 1:100, polyclonal, Atlas Antibodies), Rho GDP-dissociation inhibitor (RhoGDI; dilution 1:50, clone G-3, Santa Cruz Biotechnology), GPX4 (dilution 1:1000, clone EPNCIR144, Abcam, Cambridge, MA, USA), and FTH1 (dilution 1:400, clone EPR3005Y, Abcam).

The evaluations of IHC slides were performed as follows. For AR, the percentage of tumor cells with nuclear expression was calculated as previously described.[30] According to the previous report,[30] cases with ≥ 10% of expression were

considered as AR positive and the others were considered as AR negative. The expression of CD56, synaptophysin and chromogranin A was assessed as previously described,[31] and cases with > 10% of expression in tumor cells were considered as positive.

The nuclear expression of p53 was categorized as wild type and mutant pattern as previously described.[32] PTEN expression was assessed by comparing the staining between tumor and adjacent normal glands or stroma as previously described.[33] Nuclear expression of QKI was graded as 4 categories compared with the expression in adjacent stromal fibroblasts and finally dichotomized to low and high expression as previously described.[20] The IHC of ITGB4 was evaluated as low and high expression. Compared with the expression of adjacent nerves, cases with equal or stronger diffuse cytoplasmic staining in > 30% of tumor cells were considered as high ITGB4 expression.[34] The expression of MPRIP and GPX4 was evaluated with 50% cut-off value as previously described.[35] As previously described,[36] at least 50% of tumor cells with RhoGDI moderate intensity were considered as high expression. The cytoplasmic expression of FTH1 with > 75% of tumor cells was considered as high expression as previously described.[37]

13. Statistical analysis

Statistical calculation was performed with SPSS version 21.0 (IBM, Chicago, IL, USA). The relationships between two cell line groups and the expression values obtained by microRNA array were analyzed using Welch's ANOVA test. The associations between microRNA expression values and the other genes were analyzed by using Pearson correlation test. For the comparison of patients' age, student's t-test was used. PFS was estimated by the Kaplan-Meier method with log-rank test. Multivariate regression was analyzed using the Cox proportional hazards model. Significance statements referred to P-values of two-tailed tests < 0.05.

III. RESULTS

1. MicroRNA-200 family are downregulated in DNPC

Previous transcriptomic analysis of metastatic CRPCs have identified AR and NE scoring gene sets that can classify ARPC, neuroendocrine prostate cancer (NEPC) and DNPC.[2] To redefine established prostate cancer cell lines into ARPC, NEPC and DNPCs, the AR and NE scoring gene sets were applied to CCLE RNA-sequencing dataset (Figure 1A). A heatmap of the gene sets revealed three groups accordingly: 22RV1, VCaP, LNCaP and MDA-PCa-2B cells as ARPC, NCI-H660 cell as NEPC and PC3 and DU145 cells as DNPC. Since VCaP and 22RV1 cells expressed some NE markers, LNCaP and MDA-PCa-2B cells were selected as models of ARPC and PC3 and DU145 cells were selected as model of DNPC.

Then, comparison of microRNA expression profiles between LNCaP and PC3 cells was performed by microRNA array. Fifty-seven of 888 (6.4%) microRNAs were significantly overexpressed, and 23 (2.6%) microRNAs were significantly under-expressed in PC3 cell compared to LNCaP cell (Log2 fold difference > 2, $P < 0.05$). Notably, all the five miR-200 family (miR-141, -200a/b/c and -429) were ranked as top overexpressed microRNAs in LNCaP cell (Figure 1B).

2. QKI, a microRNA-200 family target gene, is overexpressed in DNPC

Since under-expression in DNPC was noted to all five members of miR-200 family, search for a common target gene was performed. There were 218 putative target genes shared by two broadly conserved miR-200b, -200c, -429 and miR-141, -200a subfamilies (Figure 2A). Using the human dataset as a filter, these putative target genes were narrowed down to 12 genes that showed inverse expressional correlations with miR-200 families. The top rank (inverse correlation) gene was QKI and it was the only gene overexpressed in PC3 and DU145 cells compared to other cell lines (Figure 2A). The overexpression of QKI was confirmed in PC3 cells by Western blot (Figure 2B). When comparing the five miR-200 families' ability to inhibit QKI expression in PC3 cell, miR-200b showed the most significant repression of QKI expression in PC3 cell (Figure 2C).

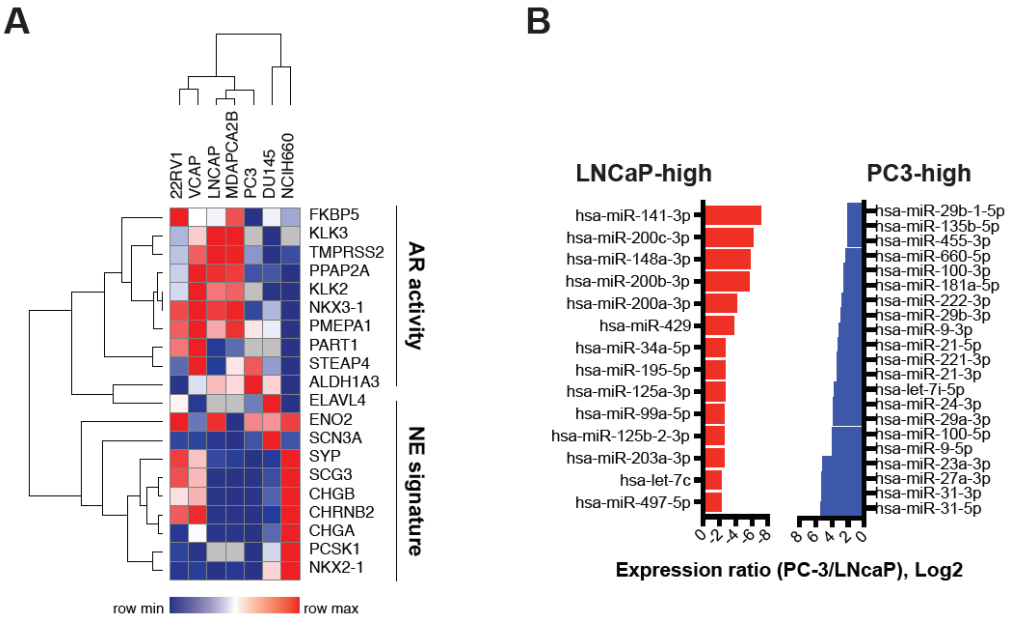

Figure 1. miR-200 family are enriched in double negative prostate cancer (DNPC). (A) PC3 and DU145 cells were selected as cell line model of DNPC after hierarchical clustering by using androgen receptor (AR) activity and neuroendocrine (NE) signature associated genes. (B) Top overexpressed microRNAs in LNCaP and PC3 cells were displayed.

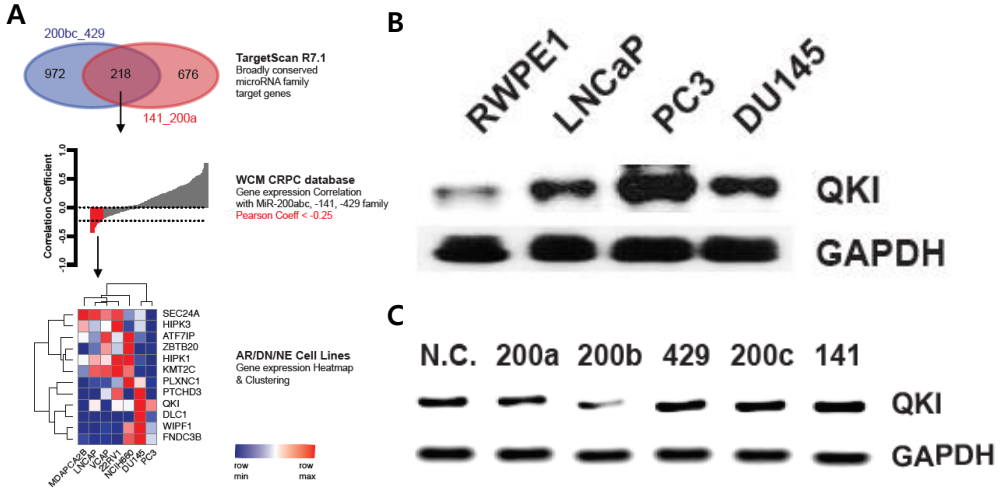

Figure 2. miR-200 family target QKI is enriched in double negative prostate cancer

(DNPC). (A) miR-200 familial target mRNA prediction by TargetScan. Two groups of putative target mRNAs by miR-200b, 200c, 429 and miR-141, 200a were combined, resulting 218 genes overlapped. Then their expressional correlation with miR-200 family score in the Weil-Cornell Medicine castration-resistant prostate cancer database was calculated. Using -0.25 as cut-off value, selected 12 genes expression was analyzed in prostate cancer cell lines. Genes and cells were clustered to show the distributional relationship. (B) PC3 and DU145 cells overexpressed QKI compared to LNCaP and RWPE-1 cells in Western blot. (C) After treating PC3 cell with miR-200 family for 48 hours, the expression of QKI was assessed in Western blot. Among miR-200 family, miR-200b repressed the expression of QKI most.

3. Clinicopathologic characteristics of DNPC

To identify DNPC, IHC for AR and NE markers was performed in prostate cancer tissue specimen. The expression of AR was dichotomized as positive and negative with cut-off value of 10% as previously described.[30] Among 72 CRPC cases, 16 cases were classified as AR negative and the others showed AR positivity. All of 83 ADT-naïve PCs showed AR positivity (Figure 3). None of cases showed NE marker expression > 10% of tumor cells. Considering the expression of AR and NE markers, 72 CRPC cases divided as 16 DNPCs and 56 ARPCs (Figure 4).

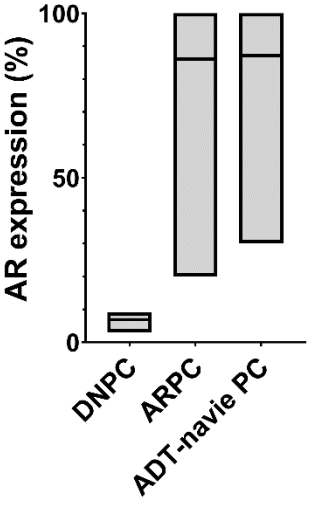

Figure 3. The differences in androgen receptor (AR) expression according to the prostate cancer subtype. Compared to AR positive prostate cancer (ARPC) and androgen deprivation therapy-naïve prostate cancer (ADT-naïve PC), all double negative prostate cancers (DNPCs) showed < 10% of AR expression.

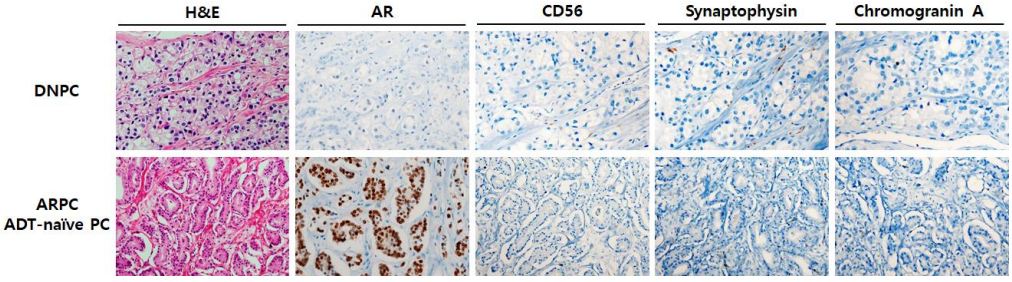

Figure 4. The immunohistochemical profiles of double negative prostate cancer (DNPC), androgen receptor positive prostate cancer (ARPC) and androgen deprivation therapy-naïve prostate cancer (ADT-naïve PC).

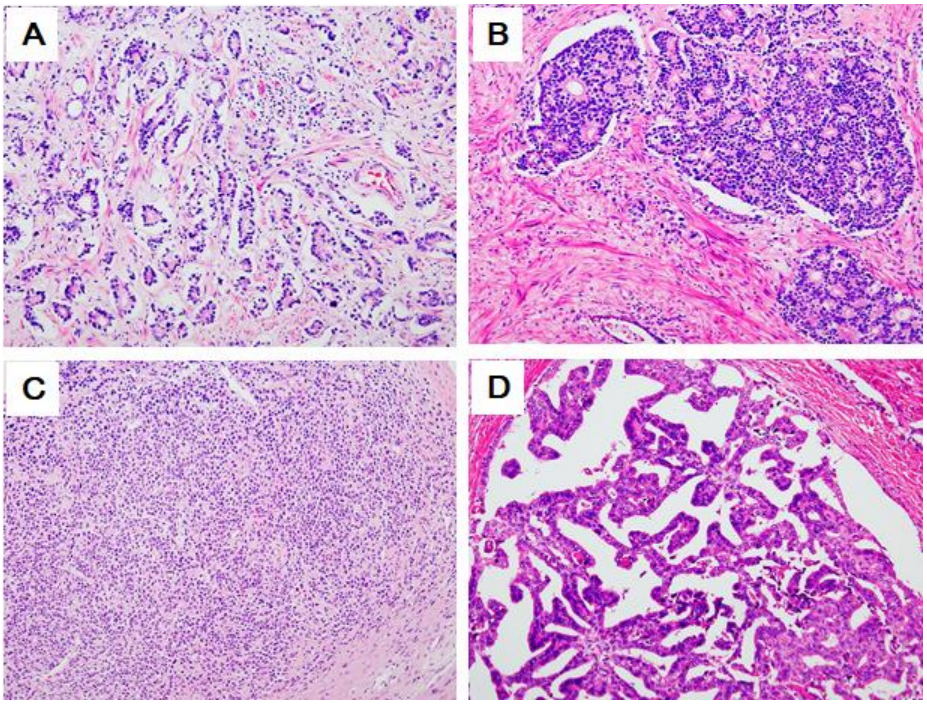

Figure 5. Various morphologic features of double negative prostate cancer (DNPC). (A) Among 16 DNPCs, 3 cases showed Gleason score 7, which belonged International Society of Urological Pathology (ISUP) grade group 2. (B) Other cases showed Gleason score 7 to 10, which belonged to ISUP grade group 3 to 5. (C) Some cases which belonged to ISUP grade group 5 showed solid growth pattern. (D) Two DNPCs showed ductal type adenocarcinoma component in 5 to 10% of entire tumor.

Sixteen DNPCs showed various morphologic features. Three cases showed Gleason score 7, which belonged to ISUP grade group 2 and others showed Gleason score 7 to 10, which belonged to ISUP grade group 3 to 5. Some cases which belonged to ISUP grade group 5 showed solid growth pattern. Two DNPC cases were mixed type adenocarcinoma showing ductal type adenocarcinoma in 5 to 10% of entire tumor (Figure 5). When comparing several clinicopathologic parameters according to prostate cancer subtype, DNPC showed significant correlation with several clinicopathologic parameters (Table 1): tumor volume > 5cc ($P < 0.001$), presence of SVI ($P < 0.001$), presence of RM extension ($P = 0.008$), presence of LVI ($P < 0.001$), presence of lymph node metastasis ($P = 0.001$) and presence of disease progression ($P < 0.001$).

Then, IHC for QKI, p53 and PTEN was performed to evaluate the immunohistochemical profiles according to the subtypes of prostate cancer (Table 2 and Figure 6). On QKI IHC, 8 out of 16 (50.0%) DNPCs showed high QKI expression, while 4 out of 52 (7.1%) ARPCs and 4 out of 83 (4.8%) ADT-naïve PCs showed high QKI expression ($P < 0.001$). In addition, higher proportion of p53 mutant pattern was identified in DNPC (68.8%) than ARPC (14.3%) and ADT-naïve PCs (18.1%, $P < 0.001$). However, loss of PTEN expression was not significant according to the subtypes of prostate cancer ($P = 0.620$).

Table 1. Clinicopathological characteristics 155 prostate cancer patients according to the prostate cancer subtype

Category	Variables	No. of cases (*n*=155)	DNPC (%) (*n*=16)		ARPC (%) (*n*=56)		ADT-naïve PC (%) (*n*=83)		*P*-value
Age (y)*	≤ 66	75	8	(50.0)	30	(53.6)	37	(44.6)	0.577
	> 66	80	8	(50.0)	26	(46.4)	46	(55.4)	
ISUP grade group	2	48	3	(18.7)	17	(30.4)	28	(33.7)	0.531
	3-5	107	13	(81.3)	39	(69.6)	55	(66.3)	
Tumor volume	≤5cc	126	3	(21.4)	47	(83.9)	76	(91.6)	< 0.001
	>5cc	27	11	(78.6)	9	(16.1)	7	(8.4)	
EPE	Absent	58	2	(14.3)	21	(37.5)	35	(42.2)	0.138
	Present	95	12	(85.7)	35	(62.5)	48	(57.8)	
SVI	Absent	136	3	(21.4)	51	(91.1)	82	(98.8)	< 0.001
	Present	17	11	(78.6)	5	(8.9)	1	(1.2)	
RM extension	Absent	55	3	(21.4)	13	(23.2)	39	(47.0)	0.008
	Present	98	11	(78.6)	43	(76.8)	44	(53.0)	
LVI	Absent	140	2	(14.3)	55	(98.2)	83	(100)	< 0.001
	Present	13	12	(85.7)	1	(1.8)			
Pathologic T stage	pT2	58	2	(14.3)	21	(37.5)	35	(42.2)	0.138
	pT3 and pT4	95	12	(85.7)	35	(62.5)	48	(57.8)	
LNM	Absent	43	2	(40.0)	15	(93.7)	26	(100)	0.001
	Present	4	3	(60.0)	1	(6.3)			
Disease progression	Absent	79					79	(95.2)	< 0.001
	Present	76	16	(100)	56	(100)	4	(4.8)	

Abbreviations: DNPC, double negative prostate cancer; ARPC, androgen receptor positive prostate cancer; ADT-naïve PC, androgen deprivation therapy-naïve prostate cancer; ISUP, International Society of Urological Pathology; EPE, extraprostatic extension; SVI, seminal vesicle involvement; RM, resection margin; LVI, lymphovascular invasion; LNM, lymph node metastasis

*The median age was 66.0 years.

**Tumor volume, extraprostatic extension, seminal vesicle involvement, resection margin extension, lymphovascular invasion and pathologic T stage were evaluated in 153 cases. Lymph node was evaluated in 47 cases

Table 2. Immunohistochemical staining results of QKI, p53 and PTEN according to the prostate cancer subtype

Category	Variables	No. of cases (*n*=155)	DNPC (%) (*n*=16)		ARPC (%) (*n*=56)		ADT-naïve PC (%) (*n*=83)		*P*-value
QKI expression	Low	139	8	(50.0)	52	(92.9)	79	(95.2)	< 0.001
	High	16	8	(50.0)	4	(7.1)	4	(4.8)	
p53 expression	Wild type pattern	121	5	(31.2)	48	(85.7)	68	(81.9)	< 0.001
	Mutant pattern	34	11	(68.8)	8	(14.3)	15	(18.1)	
PTEN expression	Intact	52	4	(25.0)	21	(37.5)	27	(32.5)	0.620
	Loss	103	12	(75.0)	35	(62.5)	56	(67.5)	

Abbreviations: DNPC, double negative prostate cancer; ARPC, androgen receptor positive prostate cancer; ADT-naïve PC, androgen deprivation therapy-naïve prostate cancer; QKI, quaking; PTEN, phosphatase and tensin homolog

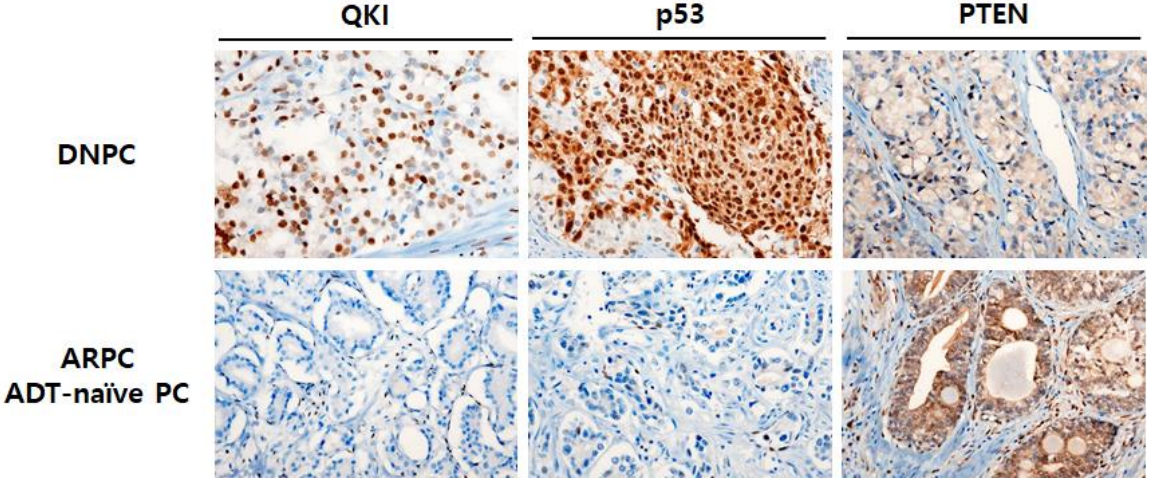

Figure 6. The characteristic immunohistochemical features of double negative prostate cancer (DNPC). DNPC showed high QKI expression and mutant pattern of p53. No significant difference was identified in PTEN immunohistochemical staining.

4. QKI overexpression enhances stemness and EMT

Recent study showed that miR-200c targeting QKI in multiple types of epithelial cancers which linked to EMT and metastatic progression. In addition, QKI overexpression in metastatic versus primary tumors as well as poorly differentiated versus well differentiated primary tumor was confirmed on multiple prostate cancer datasets.[19] Based on these findings, a hypothesis that QKI may promote stemness and trigger a transition from ARPC to DNPC was made. By using CRISPR-Cas9 complex,[27] LNCaP and MDA-PCa-2B QKI-OE cells were generated. The sphere formation assay revealed increased numbers and sizes of spheres formed by QKI-OE cells (Figure 7A). In addition, ALDH active cell population increased in QKI-OE cells, implying increased stemness in QKI-OE cells (Figure 7B).

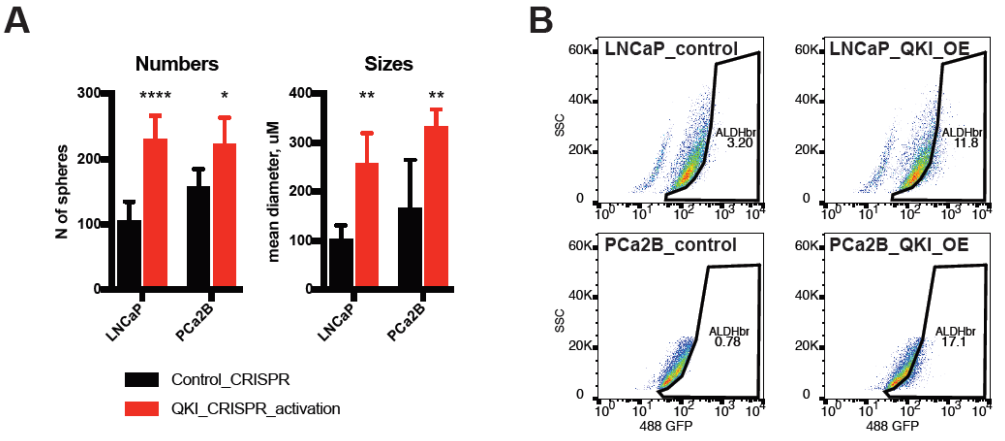

Figure 7. QKI promotes stemness. (A) Tumor sphere formation assays of QKI-overexpressing (QKI-OE) cells and control cells. LNCaP or MDA-PCa-2B (PCa2B) cells of modified QKI expressions by CRISPR-mediated-transcriptional-activation were cultured in serum-free tumor sphere media at ultra-low attachment 12-well plates. Tumor spheres were measured after 10 days. Number (left) and mean diameter (right) of spheres were significantly different between control group and QKI-OE cells ($^{*}P < 0.05$; $^{**}P < 0.01$; $^{****}P < 0.001$). (B) ALDH-active cell (ALDHbr) populations in QKI-overexpressing LNCaP (upper) and PCa2B (lower) cells. ALDHbr population gate was set by diethylaminobenzaldehyde treated cells. Then the

proportion of ALDHbr population was measured in QKI-OE cells and control cells.

Then, RNA-sequencing on QKI-OE DU145 cells was performed to validate the differences in the expression of EMT and stemness marker according to the QKI expression status. RNA-sequencing data showed the upregulation of *ARHGDIA* and *ITGB4* compared to the control group (Figure 8). To confirm the RNA-sequencing data of QKI-OE DU145 cells, the RNA-sequencing data of SU2C-PCF dataset[26] was analyzed. Similar to RNA-sequencing data of QKI-OE DU145 cells, SU2C-PCF dataset showed significant overexpression of *QKI* and *ITGB4* in DNPC compared to ARPC and NEPC (Figure 9).

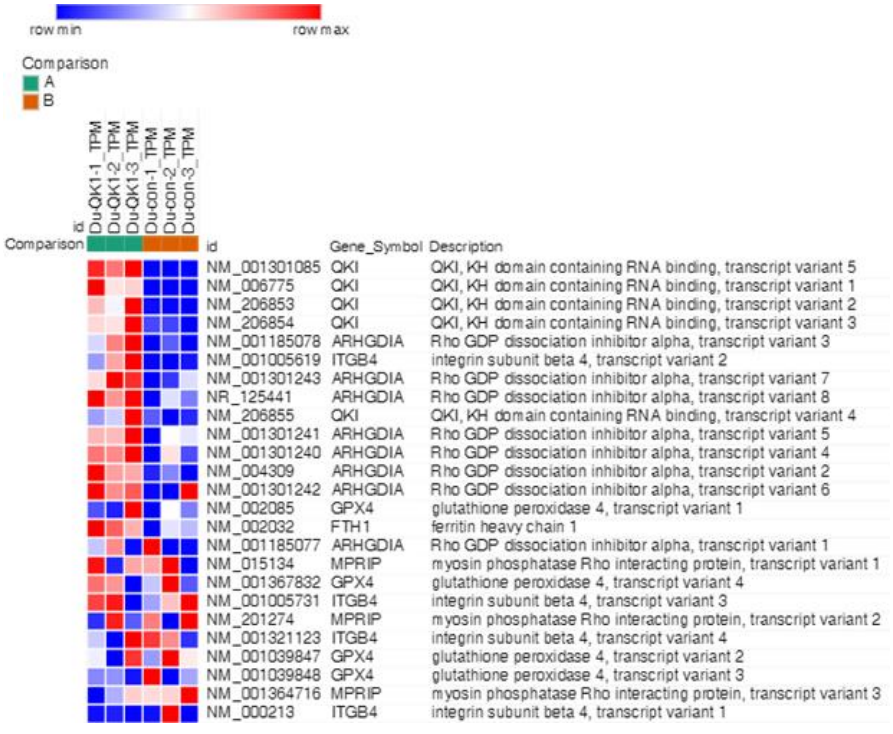

Figure 8. The RNA-sequencing data of DU145 cells according to QKI expression status. By RNA-sequencing data analysis, the expression of several genes associated with epithelial-to-mesenchymal transition and stemness was assessed. Compared to the control group, the upregulation of *ARHGDIA* and *ITGB4* was identified in QKI-overexpressing cells.

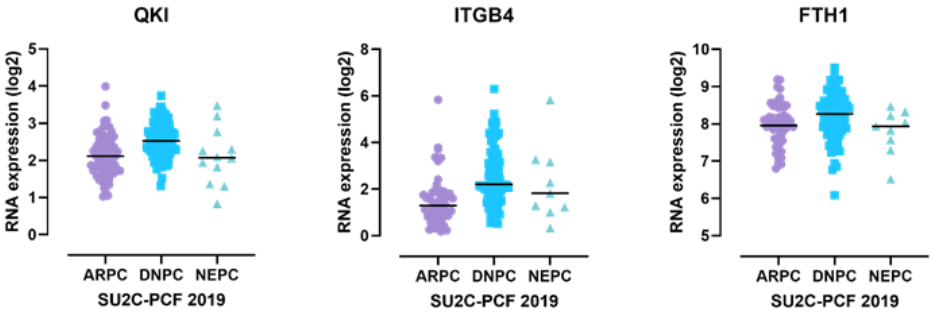

Figure 9. The comparison of RNA expressions among androgen receptor positive prostate cancer (ARPC), double negative prostate cancer (DNPC) and neuroendocrine prostate cancer (NEPC) of Stand Up to Cancer/Prostate Cancer Foundation (SU2C-PCF) dataset. In SU2C-PCF dataset, DNPC showed significant expression of *QKI* (P < 0.001), *ITGB4* (P < 0.001) and *FTH1* (P = 0.033) expression compared to ARPC and NEPC.

From the RNA-sequencing data obtained from SU2C-PCF dataset and QKI-OE DU145 cells, RhoGDI and ITGB4 were selected as markers for IHC. In addition, IHC for MPRIP, encoded by *MPRIP* gene directly targeted by QKI[19] was also performed (Figure 10). When analyzing the expression of RhoGDI, MPRIP and ITGB4 according to the QKI expression status, high expression of RhoGDI, MPRIP and ITGB4 was significantly identified in cases with high QKI expression (Table 3; P = 0.014, < 0.001 and < 0.001, respectively).

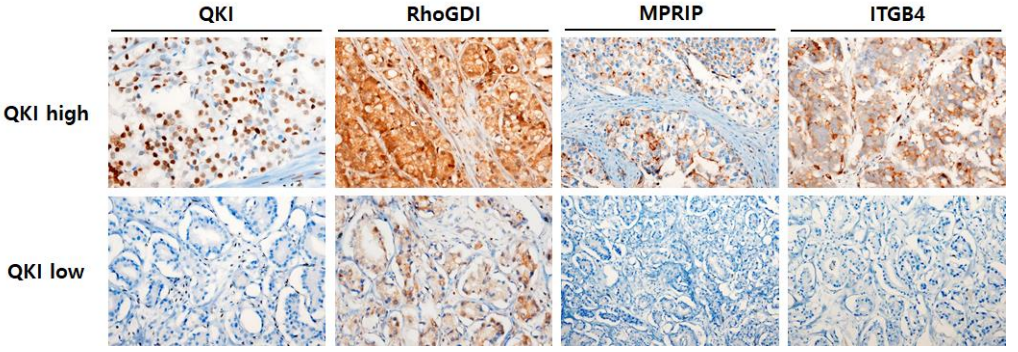

Figure 10. The expression of Rho guanine nucleotide dissociation inhibitor (RhoGDI),

myosin phosphatase rho interacting protein (MPRIP) and integrin beta 4 (ITGB4) according to QKI expression status. Compared to cases with low QKI expression, those with high QKI expression showed high expression of RhoGDI, MPRIP and ITGB4.

Table 3. Immunohistochemical staining results of RhoGDI, MPRIP and ITGB4 according to QKI expression status

Category	Variables	No. of cases (*n*=155)	QKI high (%) (*n*=16)		QKI low (%) (*n*=139)		*P*-value
RhoGDI expression	Low	74	3	(18.8)	71	(51.1)	0.014
	High	81	13	(81.3)	68	(48.9)	
MPRIP expression	Low	132	7	(43.8)	125	(89.9)	< 0.001
	High	23	9	(56.3)	14	(10.1)	
ITGB4 expression	Low	146	9	(56.3)	137	(98.6)	< 0.001
	High	9	7	(43.8)	2	(1.4)	

Abbreviations: RhoGDI, Rho guanine nucleotide dissociation inhibitor; MPRIP, myosin phosphatase rho interacting protein; ITGB4, integrin beta 4; QKI, quaking

5. QKI-OE prostate cancer is associated with hypercholesterolemia and selectively inhibited by fluvastatin

Several studies have reported the association between prostate cancer and hypercholesterolemia and BMI.[38,39] Since QKI regulates lipid metabolism,[13,14] the association between QKI expression and serum cholesterol level or BMI was investigated in 163 prostate cancer patients. Cases with high QKI expression showed significantly higher serum cholesterol level than those with low QKI expression (P = 0.020; Figure 11A). However, no significant difference was observed between QKI expression and BMI (P = 0.428; Figure 11B).

Then, *in silico* drug screening was performed to identify the therapeutic agent of QKI. Among the drugs that showed inverse correlation with QKI expression, top hits included the GPX4 inhibitors such as ML210 and ML162 and 3-hydroxy-3-methyl-glutaryl-coenzyme A (HMG-CoA) reductase inhibitors (statins) such as fluvastatin and lovastatin (Figure 12A). However, the GPX4 inhibitors are not yet available *in vivo*. Instead, the statins were selected as therapeutic agent of QKI since high QKI expression and hypercholesterolemia were significantly associated in prostate cancer patients.

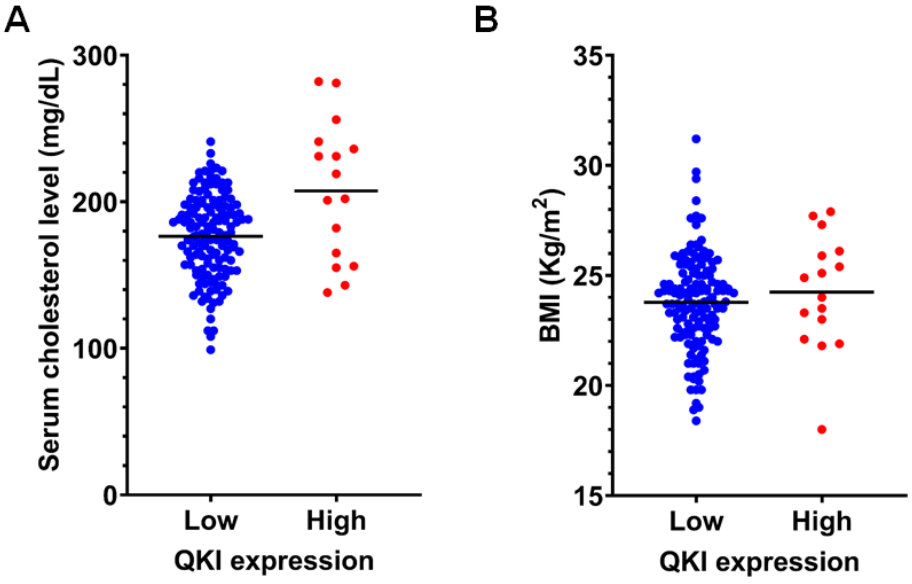

Figure 11. The distribution of serum cholesterol level and body mass index (BMI) according to QKI expression status. (A) Cases with high QKI expression showed higher serum cholesterol level than those with low QKI expression (P = 0.020). (B) No significant difference was identified according to QKI expression status (P = 0.428).

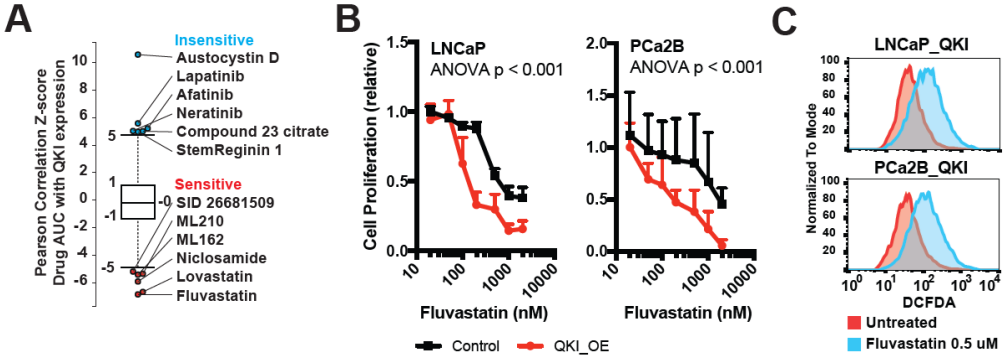

Figure 12. QKI-overexpressing (QKI-OE) cells are selectively vulnerable to statins. (A) Using Cancer Therapeutic Response Portal database, drug sensitivity (AUC) correlation with QKI gene expression was calculated. (B) QKI-OE LNCaP and MDA-PCa-2B (PCa2B) cells were treated with fluvastatin. At 5 days after fluvastatin treatment, cells were harvested and counted. Relative cell proliferation compared to control group was displayed. (C) Compared to

control group, intracellular reactive oxygen species increased in QKI-OE LNCaP and PCa2B cells after treating fluvastatin.

When treating QKI-OE LNCaP and MDA-PCa-2B cells with fluvastatin, the proliferation of QKI-OE cells diminished compared to control group (Figure 12B). In addition, the intracellular ROS increased after treating fluvastatin on QKI-OE LNCaP and MDA-PCa-2B cells (Figure 12C). From these findings, the increased sensitivity of QKI-OE cells to GPX4 inhibitors and statins may be related to intracellular lipid hydroperoxide accumulation and ferroptosis.[40]

Next, the differences in the expression of several reported genes associated with lipid metabolism and ferroptosis[11] were investigated by RNA-sequencing. Among these genes, the expression level of *FTH1* (Figure 8) and *ACSL4* transcript variant 3 and 4 (Figure 13) significantly differed between QKI-OE DU145 cells and control group. In addition, SU2C-PCF dataset showed significant overexpression of FTH1 in DNPC than other subtypes (Figure 9). This finding indicated that the regulation of QKI affected on the activity of ferroptosis.

To investigate the relationship between QKI overexpression and ferroptosis in tissue specimen, the expression of GPX4 and FTH1 was evaluated by IHC (Figure 14 and Table 4). Compared to QKI low cases, QKI high cases showed frequently low GPX4 expression ($P < 0.001$) and high FTH1 expression ($P = 0.002$).

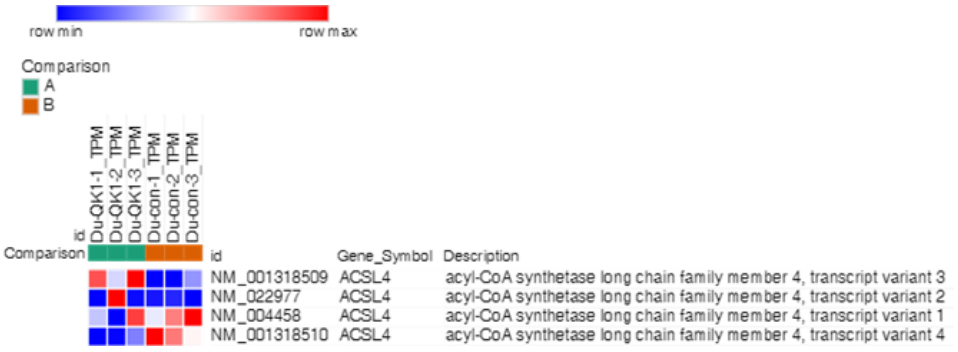

Figure 13. The expression level of *ACSL4* transcript variant between QKI-overexpressing (QKI-OE) DU145 cells and control group. Compared to control group, *ACSL4* transcrpit variant 3 was significantly upregulated in QKI-OE DU145 cells. On the contrary, transcript variant 4 was significantly down-regulated in QKI-OE DU145 cells.

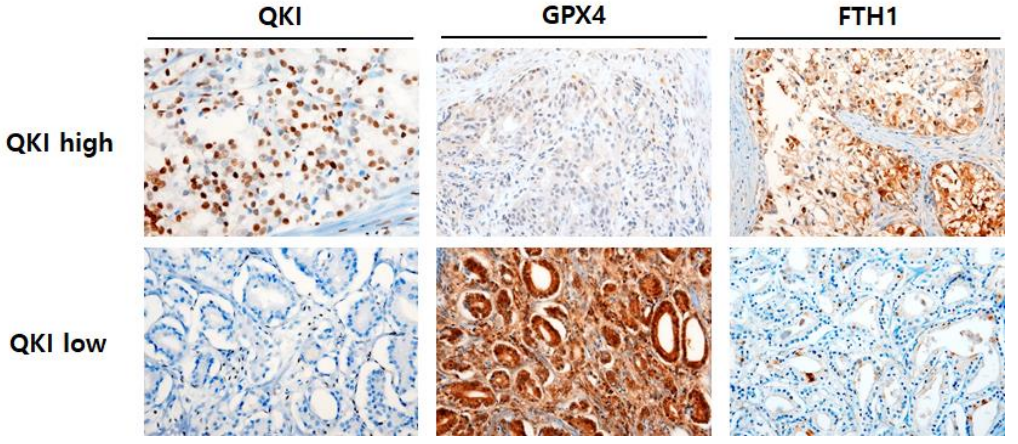

Figure 14. The expression of glutathione peroxidase 4 (GPX4) and ferritin heavy chain 1 (FTH1) according to QKI expression status.

Table 4. Immunohistochemical staining results of GPX4 and FTH1 according to QKI expression status

Category	Variables	No. of cases (*n*=155)	QKI high (%) (*n*=16)		QKI low (%) (*n*=139)		*P*-value
GPX4 expression	Low	28	8	(50.0)	20	(14.4)	< 0.001
	High	127	8	(50.0)	119	(85.6)	
FTH1 expression	Low	94	4	(25.0)	90	(64.7)	0.002
	High	61	12	(75.0)	49	(35.3)	

Abbreviations: GPX4, glutathione peroxidase 4; FTH1, ferritin heavy chain 1; QKI, quaking

6. Prognostic significance of QKI expression in DNPC

In Kaplan-Meier analysis based on the subtype, DNPC showed significantly shorter PFS compared to ARPC and ADT-naïve PC (P < 0.001; Figure 15A). In addition, cases with high QKI expression showed significantly shorter PFS than those with low QKI expression (P < 0.001; Figure 15B). When analyzing 72 CRPC cases, cases with high QKI expression showed significantly shorter PFS than those with low QKI expression (P < 0.001; Figure 15C). After combining subtype and QKI expression status in 72 CRPC cases, ARPC showed the longest PFS and DNPC with high QKI expression showed the shortest PFS (P < 0.001; Figure 15D).

Next, univariate and multivariate analysis on disease progression was performed in 72 CRPC cases to investigate the prognostic impact of several clinicophatologic factors on disease progression (Table 5). On univariate analysis, ISUP grade group 3 to 5 (P = 0.015), tumor volume > 5cc (P < 0.001), presence of EPE (P = 0.040), presence of LVI (P < 0.001), presence of SVI or lymph node metastasis (P = 0.007), DNPC with low QKI expression (P = 0.045) and DNPC with high QKI expression (P < 0.001) were significantly associated with disease progression. However, only ISUP grade group 3 to 5 (P = 0.045) and tumor volume > 5cc (P = 0.023) were significantly associated with disease progression on multivariate analysis.

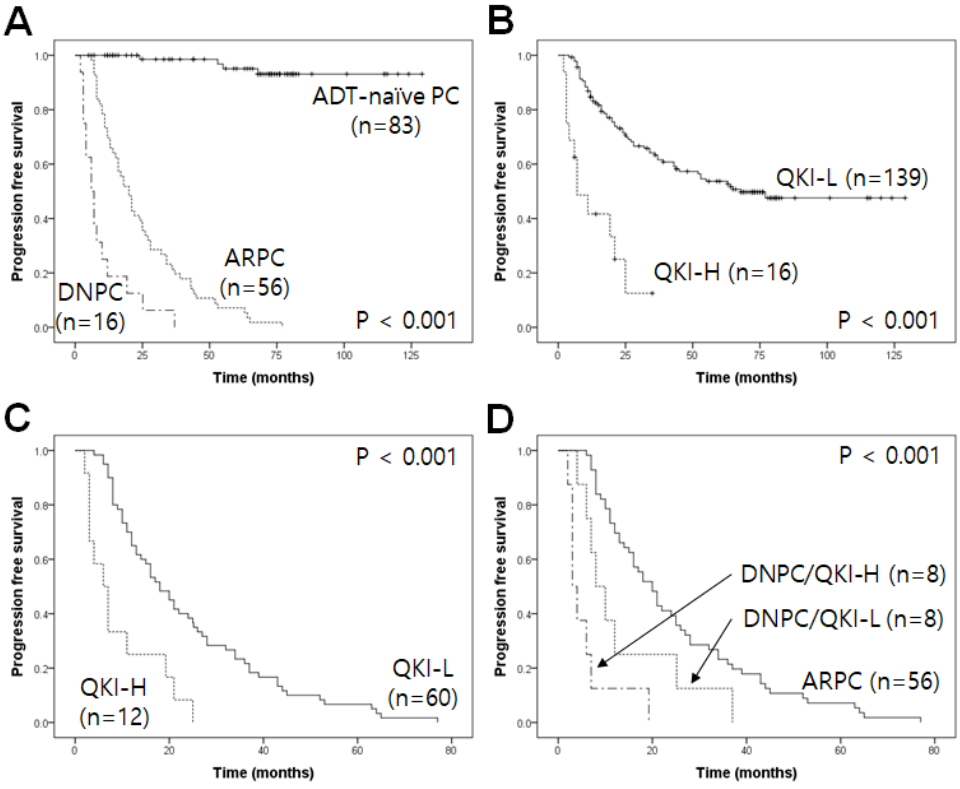

Figure 15. Progression free survival (PFS) of 155 prostate cancer patients. (A) Double negative prostate cancer (DNPC) showed shorter PFS than androgen receptor positive prostate cancer (ARPC) and androgen deprivation therapy-naïve prostate cancer (ADT-naïve PC; $P < 0.001$). (B) Cases with high QKI expression (QKI-H) showed shorter PFS than those with low QKI expression (QKI-L; $P < 0.001$). (C) When analyzing 72 castration-resistant prostate cancers (CRPCs), QKI-H cases showed shorter PFS than QKI-L cases ($P < 0.001$). (D) After classifying 72 CRPCs into 3 subgroups based on subtype and QKI expression status, DNPC with QKI-H showed the shortest PFS ($P < 0.001$).

IV. DISCUSSION

This study showed that 1) miR-200 family members were down-regulated in DNPC, while its target gene *QKI* was upregulated. 2) QKI induces stemness and EMT, promoting transition of ARPC to DNPC. 3) QKI-OE cells were selectively sensitive to

fluvastatin via the execution of ferroptosis.

DNPC showed distinct clinicopathologic characteristics compared to ARPC and ADT-naïve PCs: larger tumor volume, frequent LVI, frequent SVI, presence of lymph node metastasis and disease progression. In addition, DNPC showed frequent mutant p53 pattern. These features of DNPC partly overlaps with prostate cancer belonged to aggressive variant prostate cancer immune-infiltrative subtype according to the recently reported molecular classification.[41]

Table 5. Univariate and multivariate analysis of 72 CRPC cases on disease progression

Category	Variable	Univariate		Multivariate	
		HR(95% CI)	P-value	HR(95% CI)	P-value
Age (y)	≤ 66	1		-	
	> 66	0.967(0.604-1.546)	0.887	-	-
ISUP grade group	2	1		1	
	3-5	2.044(1.147-3.641)	0.015	1.975(1.015-3.844)	0.045
Tumor volume	≤ 5cc	1		1	
	> 5cc	3.763(2.137-6.629)	< 0.001	2.784(1.149-6.745)	0.023
EPE	Absent	1		1	
	Present	1.715(1.025-2.869)	0.040	1.021(0.550-1.896)	0.947
RM extension	Absent	1		-	
	Present	1.038(0.590-1.826)	0.897	-	-
LVI	Absent	1		1	
	Present	4.580(2.397-8.751)	< 0.001	0.292(0.029-2.906)	0.293
SVI or LNM	Absent	1		1	
	Present	2.464(1.284-4.727)	0.007	1.108(0.345-3.564)	0.863
Subtype/QKI expression	ARPC	1		1	
	DNPC/QKI-L	2.162(1.016-4.601)	0.045	5.728(0.896-36.638)	0.065
	DNPC/QKI-H	7.997(3.573-17.896)	< 0.001	4.503(0.429-47.303)	0.210

Abbreviations: CRPC, castration-resistant prostate cancer; HR, hazard ratio; CI, confidence interval; ISUP, International Society of Urological Pathology; EPE, extraprostatic extension; RM, resection margin; LVI, lymphovascular invasion; SVI, seminal vesicle involvement; LNM, lymph node metastasis; DNPC, double negative prostate cancer; QKI-L, low QKI expression; QKI-H, high QKI expression

Regulation of EMT is the important cellular function of miR-200 family.[19,42] A recent study showed that miR-200 regulates epithelial plasticity via QKI. In addition, QKI was overexpressed in metastatic prostate cancer than primary tumor.[19] Results of this study well correlated with the previous findings, except that I chose QKI by inverse

correlation with miR-200 family in metastatic CRPC dataset. In addition, increased stemness and EMT in QKI-OE cells and QKI high prostate cancer were observed, raising the possibility of transition from ARPC to DNPC by QKI. However, further studies are necessary whether QKI mediated transition can cause tumor metastasis.

Although not fully investigated, the population of DNPC has gradually increased since the widespread use of AR inhibitors of enhanced efficacies and additive androgen blockers.[43] Despite the need for DNPC as a new subset of prostate cancer, no specific therapeutic option has not been established yet.[2] Because the overexpression of QKI may promote the transition to DNPC, the inhibition of QKI may be the treatment option for DNPC patients. However, it is difficult to directly target QKI because of the various function and unclear downstream effectors of QKI.[13,15-17,19-24] Instead, targetable signaling pathway activated in QKI-OE tumors were investigated using DepMap and CTRP database. To improve target identification, the genetic interference sensitivities such as CRISPR knock-out and RNAi knock-down data were added. This approach was internally validated by checking several well established targetable drugs of specific pathways, such as BRAF and MAPK inhibitors.[44]

This study revealed that statin is a targetable drug of QKI. When treating QKI-OE cells with statin, these cells showed diminished proliferation compared with normal control. Instead, they showed increased level of intracellular ROS, suggesting the possibility of ferroptosis in QKI-OE cells triggered by lipid peroxidation. Several retrospective studies have reported the improved progression free and overall survival as well as diminished occurrence of prostate cancer with high Gleason score after application of statin.[45-47] These studies raise the possibility of applying statin as a chemotherapeutic agent. Although serum cholesterol reduction slowed tumor growth in mouse model,[48] several randomized control trials did not showed significant results. Therefore, further studies about effect of statin on prostate cancer are necessary.

In ferroptosis, p53 acts as both enhancer and suppressor. As ferroptosis enhancer, p53 inhibits the expression of solute carrier family 7 member 11 or promotes the expression of spermidine/spermine N1-acetyltransferase 1 and glutaminase 2. As

ferroptosis suppressor, p53 directly inhibits dipeptidyl peptidase 4 activity or induces the expression of cyclin dependent kinase inhibitor 1A/p21.[49] Considering the frequent p53 mutant pattern in DNPC, it is plausible to assume that the inhibitory effect on ferroptosis mediated by wild type p53 protein may be more impaired than enhancing effect. However, further study is necessary to elucidate the effect of p53 mutant protein on ferroptosis in DNPC.

Several reports investigated the ferroptosis as an option of cancer treatment and some of them focused on the GPX4, since it is the important regulator of ferroptosis.[5,11,50-52] On the contrary, the effect of statin on QKI and ferroptosis has not been fully elucidated. Instead, some speculations can be suggested based on the results of this study. First, statin itself function as a ferroptosis inducer by depleting coenzyme Q10 and inhibiting biosynthesis of GPX4.[8,9] However, in IHC of prostate cancer patients, the low expression of GPX4 was frequently observed in QKI high tumors. Thus, the effect of statin on GPX4 biosynthesis may be alleviated in cases with QKI high expression. Next, the hypothesis that statin interferes the lipid metabolism mediated by QKI can be considered. QKI regulates the expression of several enzymes related to fatty acid desaturation and elongation via PPARβ-RXRα complex.[13] If QKI is down-regulated, depletion of these enzymes may cause depletion of MUFA which reduces the sensitivity of cell to ferroptosis.[12] In addition, the altered expression of *ACSL4* promotes the lipid peroxidation of PUFA, which also triggers ferroptosis. To validate these speculations, further studies about interaction between statin and QKI, and their effect on ferroptosis are necessary.

V. CONCLUSION

This study revealed that QKI was overexpressed in DNPC and associated with poor prognosis. QKI-OE tumor cells were selectively sensitive to fluvastatin, which triggers ferroptosis. Application of statin that targets QKI can be the therapeutic option for the DNPC patients.

REFERENCES

1. Mohler JL, Antonarakis ES, Armstrong AJ, et al. Prostate Cancer, Version 2.2019, NCCN Clinical Practice Guidelines in Oncology. *J Natl Compr Canc Netw.* 2019;17:479-505.
2. Bluemn EG, Coleman IM, Lucas JM, et al. Androgen Receptor Pathway-Independent Prostate Cancer Is Sustained through FGF Signaling. *Cancer Cell.* 2017;32:474-489.e476.
3. Su W, Han HH, Wang Y, et al. The Polycomb Repressor Complex 1 Drives Double-Negative Prostate Cancer Metastasis by Coordinating Stemness and Immune Suppression. *Cancer Cell.* 2019;36:139-155 e110.
4. Bierie B, Pierce SE, Kroeger C, et al. Integrin-β4 identifies cancer stem cell-enriched populations of partially mesenchymal carcinoma cells. *Proc Natl Acad Sci U S A.* 2017;114:E2337-e2346.
5. Ghoochani A, Hsu EC, Aslan M, et al. Ferroptosis Inducers Are a Novel Therapeutic Approach for Advanced Prostate Cancer. *Cancer Res.* 2021;81:1583-1594.
6. Stockwell BR, Friedmann Angeli JP, Bayir H, et al. Ferroptosis: A Regulated Cell Death Nexus Linking Metabolism, Redox Biology, and Disease. *Cell.* 2017;171:273-285.
7. Yang WS, SriRamaratnam R, Welsch ME, et al. Regulation of ferroptotic cancer cell death by GPX4. *Cell.* 2014;156:317-331.
8. Shimada K, Skouta R, Kaplan A, et al. Global survey of cell death mechanisms reveals metabolic regulation of ferroptosis. *Nat Chem Biol.* 2016;12:497-503.
9. Viswanathan VS, Ryan MJ, Dhruv HD, et al. Dependency of a therapy-resistant state of cancer cells on a lipid peroxidase pathway. *Nature.* 2017;547:453-457.
10. Chan JJ, Kwok ZH, Chew XH, et al. A FTH1 gene:pseudogene:microRNA network regulates tumorigenesis in prostate cancer. *Nucleic Acids Res.* 2018;46:1998-2011.

11. Li Z, Chen L, Chen C, et al. Targeting ferroptosis in breast cancer. *Biomark Res.* 2020;8:58.
12. Magtanong L, Ko PJ, To M, et al. Exogenous Monounsaturated Fatty Acids Promote a Ferroptosis-Resistant Cell State. *Cell Chem Biol.* 2019;26:420-432.e429.
13. Zhou X, He C, Ren J, et al. Mature myelin maintenance requires Qki to coactivate PPARβ-RXRα-mediated lipid metabolism. *J Clin Invest.* 2020;130:2220-2236.
14. Lu H, Ye Z, Zhai Y, et al. QKI regulates adipose tissue metabolism by acting as a brake on thermogenesis and promoting obesity. *EMBO Rep.* 2020;21:e47929.
15. Conn SJ, Pillman KA, Toubia J, et al. The RNA binding protein quaking regulates formation of circRNAs. *Cell.* 2015;160:1125-1134.
16. Zong FY, Fu X, Wei WJ, et al. The RNA-binding protein QKI suppresses cancer-associated aberrant splicing. *PLoS Genet.* 2014;10:e1004289.
17. Darbelli L, Richard S. Emerging functions of the Quaking RNA-binding proteins and link to human diseases. *Wiley Interdiscip Rev RNA.* 2016;7:399-412.
18. Chen X, Liu Y, Xu C, et al. QKI is a critical pre-mRNA alternative splicing regulator of cardiac myofibrillogenesis and contractile function. *Nat Commun.* 2021;12:89.
19. Pillman KA, Phillips CA, Roslan S, et al. miR-200/375 control epithelial plasticity-associated alternative splicing by repressing the RNA-binding protein Quaking. *EMBO J.* 2018;37.
20. Kim EJ, Kim JS, Lee S, et al. QKI, a miR-200 target gene, suppresses epithelial-to-mesenchymal transition and tumor growth. *Int J Cancer.* 2019;145:1585-1595.
21. He B, Gao SQ, Huang LD, et al. MicroRNA-155 promotes the proliferation and invasion abilities of colon cancer cells by targeting quaking. *Mol Med Rep.*

2015;11:2355-2359.

22. Li F, Yi P, Pi J, et al. QKI5-mediated alternative splicing of the histone variant macroH2A1 regulates gastric carcinogenesis. *Oncotarget.* 2016;7:32821-32834.
23. Zhou X, Li X, Sun C, et al. Quaking-5 suppresses aggressiveness of lung cancer cells through inhibiting β-catenin signaling pathway. *Oncotarget.* 2017;8:82174-82184.
24. Chen AJ, Paik JH, Zhang H, et al. STAR RNA-binding protein Quaking suppresses cancer via stabilization of specific miRNA. *Genes Dev.* 2012;26:1459-1472.
25. Beltran H, Prandi D, Mosquera JM, et al. Divergent clonal evolution of castration-resistant neuroendocrine prostate cancer. *Nat Med.* 2016;22:298-305.
26. Abida W, Cyrta J, Heller G, et al. Genomic correlates of clinical outcome in advanced prostate cancer. *Proc Natl Acad Sci U S A.* 2019;116:11428-11436.
27. Konermann S, Brigham MD, Trevino AE, et al. Genome-scale transcriptional activation by an engineered CRISPR-Cas9 complex. *Nature.* 2015;517:583-588.
28. Le Magnen C, Bubendorf L, Rentsch CA, et al. Characterization and clinical relevance of ALDHbright populations in prostate cancer. *Clin Cancer Res.* 2013;19:5361-5371.
29. Seashore-Ludlow B, Rees MG, Cheah JH, et al. Harnessing Connectivity in a Large-Scale Small-Molecule Sensitivity Dataset. *Cancer Discov.* 2015;5:1210-1223.
30. Kumar V, Yu JJ, Phan V, et al. Androgen Receptor Immunohistochemistry as a Companion Diagnostic Approach to Predict Clinical Response to Enzalutamide in Triple-Negative Breast Cancer. *Jco Precision Oncology.* 2017;1:1-19.
31. Sainio M, Visakorpi T, Tolonen T, et al. Expression of neuroendocrine differentiation markers in lethal metastatic castration-resistant prostate cancer. *Pathol Res Pract.* 2018;214:848-856.

32. Yemelyanova A, Vang R, Kshirsagar M, et al. Immunohistochemical staining patterns of p53 can serve as a surrogate marker for TP53 mutations in ovarian carcinoma: an immunohistochemical and nucleotide sequencing analysis. *Mod Pathol.* 2011;24:1248-1253.

33. Morais CL, Herawi M, Toubaji A, et al. PTEN loss and ERG protein expression are infrequent in prostatic ductal adenocarcinomas and concurrent acinar carcinomas. *Prostate.* 2015;75:1610-1619.

34. Masugi Y, Yamazaki K, Emoto K, et al. Upregulation of integrin β4 promotes epithelial-mesenchymal transition and is a novel prognostic marker in pancreatic ductal adenocarcinoma. *Lab Invest.* 2015;95:308-319.

35. Guerriero E, Capone F, Accardo M, et al. GPX4 and GPX7 over-expression in human hepatocellular carcinoma tissues. *Eur J Histochem.* 2015;59:2540.

36. Wang H, Wang B, Liao Q, et al. Overexpression of RhoGDI, a novel predictor of distant metastasis, promotes cell proliferation and migration in hepatocellular carcinoma. *FEBS Lett.* 2014;588:503-508.

37. Liu NQ, De Marchi T, Timmermans AM, et al. Ferritin heavy chain in triple negative breast cancer: a favorable prognostic marker that relates to a cluster of differentiation 8 positive (CD8+) effector T-cell response. *Mol Cell Proteomics.* 2014;13:1814-1827.

38. Komaru A, Kamiya N, Suzuki H, et al. Implications of body mass index in Japanese patients with prostate cancer who had undergone radical prostatectomy. *Jpn J Clin Oncol.* 2010;40:353-359.

39. Ohno Y, Ohori M, Nakashima J, et al. Association between preoperative serum total cholesterol level and biochemical recurrence in prostate cancer patients who underwent radical prostatectomy. *Mol Clin Oncol.* 2016;4:1073-1077.

40. Comprehensive molecular characterization of urothelial bladder carcinoma. *Nature.* 2014;507:315-322.

41. Han H, Lee HH, Choi K, et al. Prostate epithelial genes define therapy-relevant prostate cancer molecular subtype. *Prostate Cancer Prostatic Dis.* 2021.

42. Burk U, Schubert J, Wellner U, et al. A reciprocal repression between ZEB1 and members of the miR-200 family promotes EMT and invasion in cancer cells. *EMBO Rep.* 2008;9:582-589.

43. Rouprêt M, Babjuk M, Burger M, et al. European Association of Urology Guidelines on Upper Urinary Tract Urothelial Carcinoma: 2020 Update. *Eur Urol.* 2021;79:62-79.

44. Johannessen CM, Johnson LA, Piccioni F, et al. A melanocyte lineage program confers resistance to MAP kinase pathway inhibition. *Nature.* 2013;504:138-142.

45. Platz EA, Leitzmann MF, Visvanathan K, et al. Statin drugs and risk of advanced prostate cancer. *J Natl Cancer Inst.* 2006;98:1819-1825.

46. Larsen SB, Dehlendorff C, Skriver C, et al. Postdiagnosis Statin Use and Mortality in Danish Patients With Prostate Cancer. *J Clin Oncol.* 2017;35:3290-3297.

47. Prabhu N, Kapur N, Catalona W, et al. Statin use and risk of prostate cancer biochemical recurrence after radical prostatectomy. *Urol Oncol.* 2021;39:130.e139-130.e115.

48. Allott EH, Masko EM, Freedland AR, et al. Serum cholesterol levels and tumor growth in a PTEN-null transgenic mouse model of prostate cancer. *Prostate Cancer Prostatic Dis.* 2018;21:196-203.

49. Kang R, Kroemer G, Tang D. The tumor suppressor protein p53 and the ferroptosis network. *Free Radic Biol Med.* 2019;133:162-168.

50. Louandre C, Marcq I, Bouhlal H, et al. The retinoblastoma (Rb) protein regulates ferroptosis induced by sorafenib in human hepatocellular carcinoma cells. *Cancer Lett.* 2015;356:971-977.

51. Eling N, Reuter L, Hazin J, et al. Identification of artesunate as a specific activator of ferroptosis in pancreatic cancer cells. *Oncoscience.* 2015;2:517-532.

52. Hao S, Yu J, He W, et al. Cysteine Dioxygenase 1 Mediates Erastin-Induced

Ferroptosis in Human Gastric Cancer Cells. *Neoplasia.* 2017;19:1022-1032.

ABSTRACT (IN KOREAN)

이중음성 전립선암에서 QKI 유전자의 발현 저하에 의한 세포 골격 안정성 및 지질막 온전성 간섭이 ferroptosis 발생에 미치는 영향

<지도교수 조남훈 >

연세대학교 대학원 의학과

박 철 근

재발성 또는 전이성 전립선암 환자들에서 안드로젠 차단 요법의 광범위한 사용은 이중 음성 전립선암의 발생을 촉진시켰다. 안드로젠 수용체 양성 전립선암에 비하여 불량한 예후를 보임에도 불구하고, 이중 음성 전립선암을 대상으로 하는 표적 치료는 아직까지 확립되지 않았다. 이번 연구에서 RNA 결합 단백질인 quaking (QKI)의 과발현이 특징인 이중 음성 전립선암에 statin을 처리하였을 때 ferroptosis가 발생하는 것을 확인하였다. PC3 및 DU145 세포주를 이중 음성 전립선암의 모델로 채택하였고 이들 세포주에서 QKI의 과발현을 확인하였다. microRNA-200 계열, 특히 miR-200b가 PC3 세포주에서 QKI의 발현을 억제하는 것 또한 확인하였다. ARPC 세포주에서 QKI를 과발현 시켰을 때, 줄기세포특성이 증가하였으며, 전립선암 조직을 대상으로 시행한 면역조직화학염색 결과, QKI의 고발현이 Rho GDP-dissociation inhibitor, myosin phosphatase rho interacting protein 및 integrin beta 4의 고발현과 연관이 있음을 확인하였다. QKI의 표적 치료제로 fluvastatin을 선택하여 QKI 과발현 세포주에 처리한 결과, 세포 증식의 감소 및 세포 내 활성 산소의 발생

증가가 관찰되었고, 이는 ferroptosis의 발생을 시사하는 소견으로 생각되었다. 생존 분석 결과, 이중 음성 전립선암 (P < 0.001)과 QKI 고발현 전립선암 (P < 0.001)은 다른 군에 비하여 불량한 무진행생존율을 보였으며, 이중 음성 전립선암과 QKI 발현을 조합하였을 때, QKI 고발현을 보이는 이중 음성 전립선암이 가장 불량한 예후를 보였다 (P < 0.001). 결론으로, QKI는 이중 음성 전립선암에서 과발현 되어 있으며, 불량한 예후와 연관이 있다. QKI 과발현 종양 세포는 fluvastatin에 잘 반응하며, 이는 ferroptosis 발생에 의한 것으로 생각된다. 따라서, QKI를 표적으로 하는 statin의 사용은 이중 음성 전립선암 환자의 치료에 있어 하나의 선택지가 될 수 있다.

핵심되는 말: 이중 음성 전립선암, quaking, ferroptosis, statin, miR-200b